J Therm Anal Calorim
DOI 10.1007/s10973-017-6298-0

Polymer blends of polyamide-6/Spandex fabric scraps and recycled poly(ethylene terephthalate)

G. A. V. Albitres[1] · L. C. Mendes[1] · S. P. Cestari[1]

Received: 28 November 2016 / Accepted: 10 March 2017

Abstract In the textile industry, scraps of natural and synthetic polymers in the shape of fibres and yarns are commonly discarded as trash. In order to follow the trends of environmental preservation, we prepared melt-extrusion blends of underwear fabric scraps—made of polyamide-6 and Spandex—and recycled poly(ethylene terephthalate) at five different proportions. The hydrogen low-field nuclear magnetic resonance analysis revealed that there was variation in the molecular mobility of the blends, indicating the interaction of the precursor polymers. The differential scanning calorimetry showed that the crystallization and melting temperatures, and the degree of crystallinity of the recycled polymers, depended on the composition of the blend. The thermogravimetric analysis showed the variation on the initial and maximum degradation temperatures according to the composition of the materials. Through the dynamic mechanical analysis, we observed two intermediate glass transition temperatures, resulting in blends with at least two phases. After selective corrosion, the SEM images revealed voids in the interfacial region of poly (ethylene terephthalate) and polyamide-6 phases. The highest elastic modulus was found for the polyamide-6/Spandex-recycled poly(ethylene terephthalate) (20/80 mass/mass%) blend. In this context, the results suggested the contribution of interchange reactions between ester–amide groups and possibly additional ones (acidolysis, alcoholysis and aminolysis) during the molten processing. The detection of two glass and melting temperatures led to deduce that polyamide-6/Spandex-recycled poly(ethylene terephthalate) formed a partially miscible blend. Thus, this work is line with the sustainability concept, and the material can be reuse for other textile applications.

Keywords Polymer blend · Recycled PET · Recycling · Recycled PA-6/Spandex · Interchange reactions

Introduction

Polymers become integral part of human life. The polymers production has remarkably grown almost 5% per year over the past 20 years in many developed countries, due to their low cost, light weight, high strength and design adaptability [1]. Polymers are continuously replacing other materials in a number of applications, and then, post-consumer wastes have grown [2]. In many applications, the products have low life cycle and are disposed in inappropriate ways, exposing people and environment to great risks. The concept of sustainability is related to cleaner production. We must assume that polymers recycling plays a paramount role in modern society, in order to reduce the impact of these residues in the environment. It is important to convert them into secondary raw materials [3]. The interest of society in environmental and sustainable issues has substantially increased the mechanical recycling of polymer waste. Until nowadays, only small amounts of polymer wastes are mechanically recycled. In most cases, the recycled polymer showed several contaminants and can have price higher than the virgin ones, since the recycling process involves costs of collection, cleaning, sorting and processing, among others [4]. The textile and clothing sectors in Brazil have great economic significance. Brazil

✉ L. C. Mendes
lcmendes@ima.ufrj.br

[1] Instituto de Macromoléculas Professora Eloisa Mano, Universidade Federal do Rio de Janeiro, Avenida Horacio Macedo,2030-Centro de Tecnologia, Bloco J, Ilha do Fundão, Rio de Janeiro 21945-970, Brazil

Published online: 20 March 2017

is the fifth largest textile industry in the world and the fourth in clothing. This sector contributes to industrial development and represents the second largest in number of employees [5]. But it generates a large amount of textile waste, which is often discarded as common trash. Synthetic fibres have a very slow degradation process—about 200 years—which is a strong reason for the reusing and recycling of textile waste [6, 7]. Polyester and polyamide are the most important synthetic polymers applied in the textile industry. Similar to polyester, nylon-6 fibre has found substantial application in the textile sector, but it is also used as engineering thermoplastic due to its excellent combination of good mechanical properties and easy processability [8, 9]. In order to give additional elasticity to the textile, Spandex^{TM}—a kind of polyurethane—is frequently woven with polyester or polyamide [10]. There are different ways of polymers recycling [11]. Concerning polymer blends, this issue presents great academic and industrial interest. Blends of polycondensation polymers have been widely studied [12–16]. Former studies on polyester/polyamide and polyamide/polyamide blends indicated that interchange reactions—as ester–amide, amide–amide, alcoholysis, acidolysis and aminolysis reactions—may have occurred during the molten processing. This process is known as reactive blending, and the interchange reactions led to produce self-compatibilizing blends through copolymers with low molecular weight [17, 18].

Blends of polyamide and polyester have academic and technological interest, but there was no study considering blends of textile waste. Therefore, this work aims to prepare melting blends of polyamide-6/Spandex (PA-6/Spandex) textile scraps and recycled poly(ethylene terephthalate)—rPET at different proportions, through reactive extrusion. The appeal of the study considers the concept of sustainability and environmental preservation. The material may meet demand for other applications.

Experimental

Materials

The rPET from carbonated beverage bottles was supplied by REPET (Uberlândia, MG, Brazil), in the shape of flakes. The scraps of PA-6/Spandex (90/10) (AMNI; 338.40 g m^{-2}; knitting; black) were kindly donated by Suspiro Intimo company (Nova Friburgo, RJ, Brazil).

Methods

The scraps of PA-6/Spandex were compression-moulded in a hydraulic press SL11 model and cooled in another hydraulic press, at 25 °C, 2.3 MPa, for 5 min, in order to obtain solid films that could be milled. The final powder was called RFA and blended with the milled flakes of rPET.

Preparation of RFA/rPET blends

The blends of RFA/rPET, at weight ratios of 100/0, 80/20, 50/50, 20/80 and 0/100, were processed in a HAAKE Rheocord torque rheometer 9000 model, at 240 °C, at 60 rpm, for 7 min. In order to minimize the hydrolysis at the high-temperature compounding, RFA and rPET were dried in an oven at 110 °C, for 12 h, and melt-processed immediately. The melt was considered homogeneous when a stable torque value was achieved inside the mixing chamber. We compression-moulded the plates of 110 × 110 × 1 mm in a hydraulic press Carver model 3851-0, at 240 °C, 2.3 MPa, during 5 min. The samples were cooled in another hydraulic press, at 25 °C, 2.3 MPa, for 5 min.

Low-field nuclear magnetic resonance (LFNMR)

The hydrogen low-field nuclear magnetic resonance analysis in solid state (^{1}H LFNMR) was performed in Maran Ultra equipment 0,54 T low field for the relaxation measurement. Proton spin–spin relaxation time (T_1H) was measured by Inversion-Recovery (p180x-t-p90x) pulse sequence. The experimental conditions were pulses $\tau = 0.1$–5000 ms, 5 s of recycle delay and 4 scans. The static and solid-state experiments were performed at 28 °C. The data were processed using WinDXP software installed in the equipment.

Thermogravimetry and thermogravimetry derivative (TG/DTG)

Thermogravimetric measurements were conducted in analyser TA Instruments Q500 model, in the range of 30–700 °C, at the rate of 10 °C min^{-1}, at nitrogen atmosphere. The thermal degradation steps were named T_{20}—degradation temperature at 20% of mass loss—T_{max}, temperature where the rate of degradation was maximum and T_{final}, final degradation temperature.

Differential scanning calorimetry (DSC)

The DSC analysis was conducted in TA equipment model Q1000, at nitrogen atmosphere, according to the ASTM D3418 [19]. The first heating cycle was performed from 0 to 270 °C, heating rate of 10 °C min^{-1}, keeping the sample at this temperature for 2 min in order to eliminate the thermal history of the sample. After that, a cooling cycle at high rate—quenching—was carried out. A second heating cycle was made at the same conditions of the first one.

Then, a second cooling cycle—from 270 to 0 °C, at the cooling rate of 10 °C min^{-1}—was conducted. Finally, a third heating cycle was made under the same conditions of the first cycle. As described in ASTM D3418, the crystalline melting temperature (T_m) was taken at the third heating cycle, and the cooling crystallization temperature (T_{cc}) was measured at the second cooling cycle. The enthalpy of crystalline fusion (ΔH_m) was used to calculate the degree of crystallinity (X_c), considering the third heating cycle, and using the theoretical melting enthalpy of 100% crystalline PA-6 and crystalline PET (190 and 136 J g^{-1}) [12, 20]. We assumed that there was 90% of PA-6 in the RFA; hence, we used this percentage to calculate the X_c of this material.

Dynamic mechanical analysis (DMA)

The storage (E') and loss moduli (E'') were determined using a dynamic mechanical analyser TA Instruments model 2980, over specimens of 170 × 125 × 3 mm at the temperature range of −80 to 100 °C, at the heating rate of 3 °C min^{-1}, frequency of 1 Hz and bending mode. The maximum of the E'' peak was used to estimate the glass transition temperature (T_g) [21–23]. Utracki and Favis [24] and Al-Jabareen et al. [13] rearranged the Fox equation [25], assuming that it can reproduce the relationship of the T_g composition in a polymeric blend PolymerA/PolymerB; in this rearrangement, one can use the experimental T_g values of the neat polymers and its blends—measured in the DMA analysis—to calculate the estimated apparent weight fraction of the PolymerA phase (w_{PolyA}) in the PolymerB-rich-phase blend, as well as to calculate the estimated apparent weight fraction of the PolymerB phase (w_{PolyB}) in the PolymerA-rich phase blend (Eq. 1),

$$w_{PolyA} = \frac{T_{g_{PolyA}}\left(T_{g_{PolyB}} - T'_{g_{PolyB}}\right)}{T'_{g_{PolyB}}\left(T_{g_{PolyB}} - T_{g_{PolyA}}\right)}$$
$$w_{PolyB} = \frac{T_{g_{PolyB}}\left(T'_{g_{PolyA}} - T_{g_{PolyA}}\right)}{T'_{g_{PolyA}}\left(T_{g_{PolyB}} - T_{g_{PolyA}}\right)} \quad (1)$$

As proposed by Santana et al. [26] and Al-Jabareen et al. [13] and applied by Mendes and Pereira [15] in blends of poly(ethylene terephthalate)/polycarbonate (PET/PC), the degree of effectiveness (e_d) was calculated in an attempt to understand the interaction between the blend components (Eq. 2),

$$e_{d_{PolyA}} = \frac{w_{PolyA} \times x_{PolyB}}{\left(w_{PolyA} \times x_{PolyB}\right) + \left(\left(1 - w_{PolyB}\right) \times x_{PolyA}\right)} \times 100$$
$$e_{d_{PolyB}} = \frac{w_{PolyB} \times x_{PolyA}}{\left(w_{PolyB} \times x_{PolyA}\right) + \left(\left(1 - w_{PolyA}\right) \times x_{PolyB}\right)} \times 100 \quad (2)$$

where $x_{polyA/B}$ is the weight fraction of PolymerA/B in the blend.

Scanning electron microscopy (SEM)

The SEM images were captured by a SEM Fei Quanta 400 equipment, voltage of 20 kV, from the transversal surface obtained by fracturing the specimen in liquid nitrogen. The selective extraction—etched with acetic acid—was made in order to reveal the interfacial region of the blend [27, 28].

Tensile test

The tensile test was carried on a EMIC equipment DL 2000 model according to ASTM-D882 [29], with load cell of 20 kN, speed of 5 mm min^{-1}, over specimens of 100 × 10 × 1 mm. The elastic modulus, stress and elongation at break were determined. The results (Table 5) were expressed using the median curve of, at least, 5 specimens for each blend.

Results and discussion

DMA

According to the literature, the miscibility of a polymer blend may be evaluated by using dynamic mechanical analysis (DMA). Some authors defined that polymer blend comprises systems with total miscibility, partial miscibility, or totally immiscible, according to the glass transition temperature (T_g). If the blend shows a unique T_g, the blend is considered miscible; if it maintains the T_g of the precursor polymers, it is named immiscible; if both T_g displaces along the temperature axis, the blend is known as partially miscible [21–23, 30].

As mentioned before, polycondensation polymers may react to each other when processed in the molten state. Interchange reactions—as ester–amide, alcoholysis, acidolysis and aminolysis (Schemes 1–4)—may happen, producing block and random copolymers [31–36]. The arising of these entities depends on the composition of the blend, the viscosity of the precursor polymers, temperature, speed and time of processing, among others [37]. These copolymers acted as compatibilizing agent, reducing the interfacial energy between phases.

The results on miscibility of blends, related to polycondensation polymers, are not convergent. Lee et al. [38] mentioned the immiscibility of the blend PA-6/PET (80/20). Through NMR studies Utracki and Favis [24] confirmed the occurrence of interchange reactions between

Scheme 1 Reaction mechanism of ester–amide interchange reaction

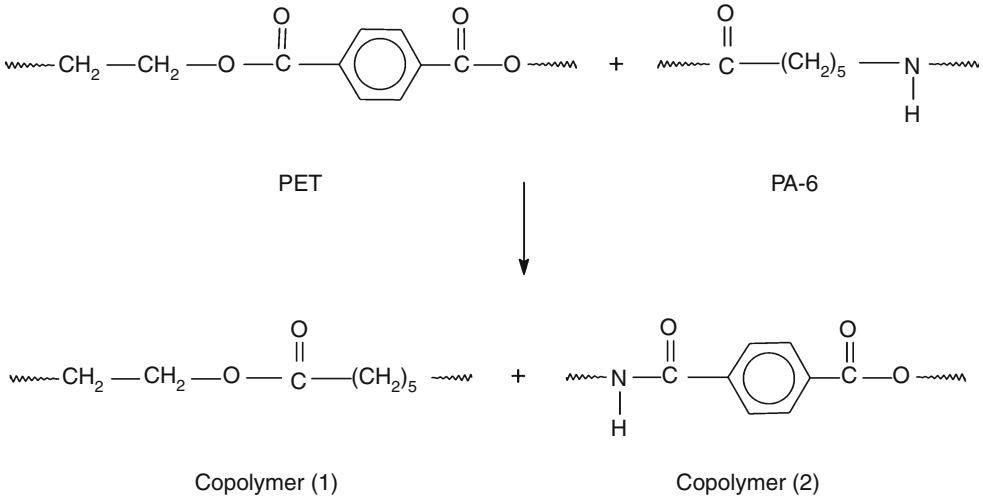

Scheme 2 Reaction mechanism of alcoholysis

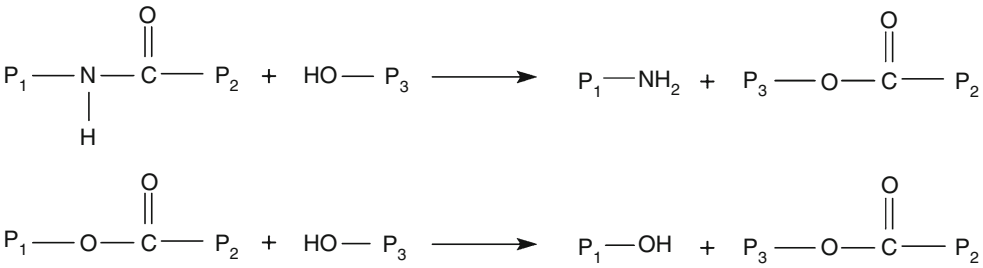

Scheme 3 Reaction mechanism of acidolysis

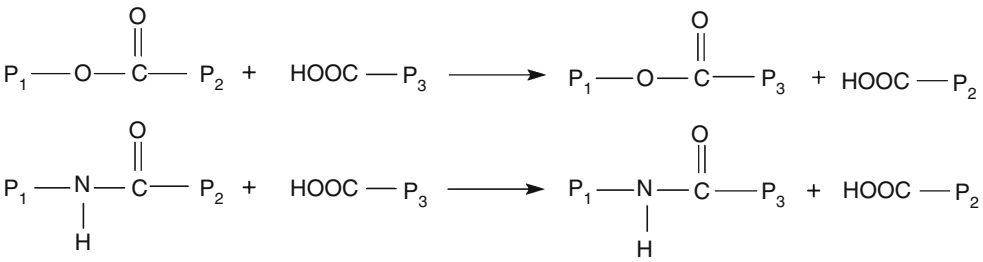

Scheme 4 Reaction mechanism of aminolysis

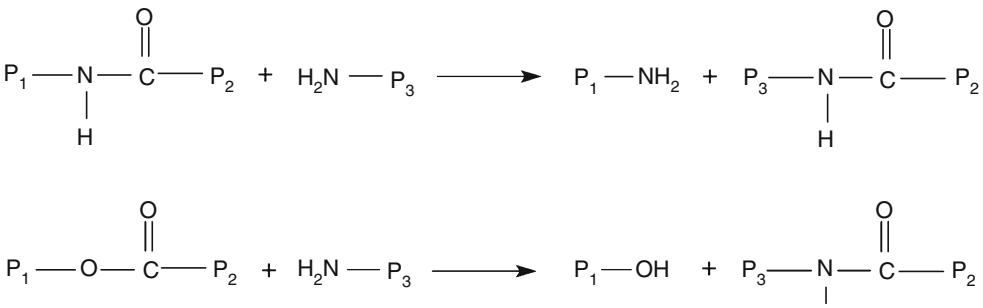

PET/PA-6 blend in the molten state. These reactions were also described by Mendes et al. [39] in the investigation of reactive extruded PET/polycarbonate blends. The authors reported the variation of T_g of the parent polymers according to the composition and the formation of partially miscible blends.

Figures 1 and 2 show the storage modulus (E') and loss modulus (E'') of the precursor polymers and blends. Table 1 shows the T_g of the materials. Dissimilar behaviour was noticed below and above 0 °C. Below 0 °C, RFA and the blends showed E' higher than rPET, while reverse behaviour was observed above 0 °C. It is interesting to

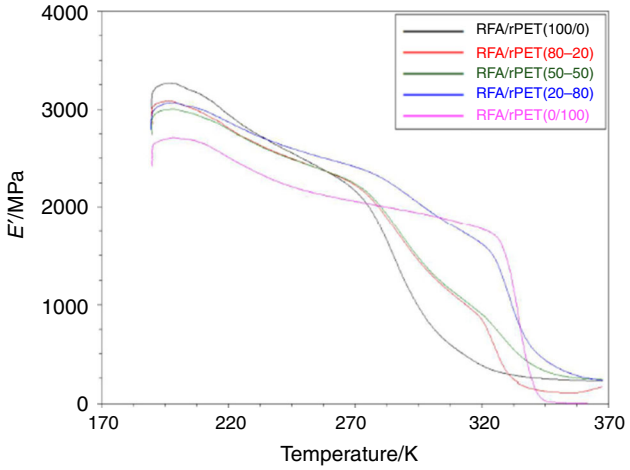

Fig. 1 Overlay of the storage moduli (E') of RFA/rPET materials

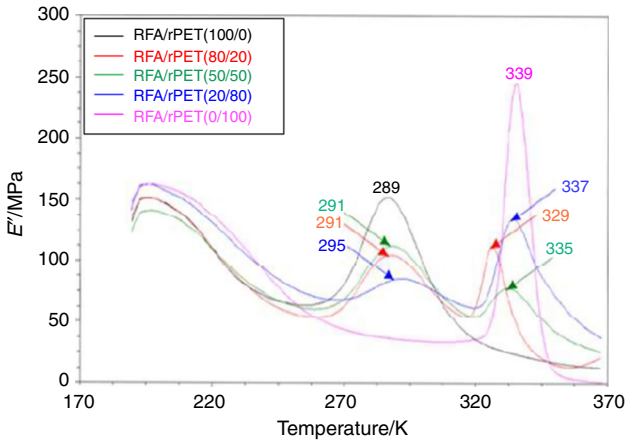

Fig. 2 Overlay of the loss moduli (E'') of RFA/rPET materials

notice that the blend RFA/rPET (20/80) showed E' superior to the rPET. The loss modulus curves evidenced the relaxation process related to the glass transition temperature (T_g). In this work, the RFA is a blend of PA-6 and Spandex. And Spandex is a segmented polyurethane that, when coating polyamide fibres, offers the feasibility of elastic recovery to the yarn. There are several articles on blends of PA-6 and polyurethane [40–45]. Only one of them (John et al. [44]) reported on the T_g related to the coating of polyurethane on PA-6 fibres. They showed a slight decrease on the PA-6 T_g in the presence of polyurethane. The RFA (PA-6/Spandex^{TM}) used herein showed a unique T_g (16 °C). We believe that the melt processing fostered the compatibility of the two components, due to the formation of hydrogen bond between PA-6 amide groups and urethane groups of the Spandex^{TM}. Herein, the maximum of E'' peaks revealed that the blends (RFA/rPET) showed two T_g between the ones of the precursor polymers. According to the values in Table 1, both T_g were shifted as function of the composition of the blend. A slight increase for RFA and a significant reduction for rPET were noticed. We can deduce that the variation of the T_g was due to the interchange reactions during the melt processing. The block copolymer emerged from these reactions and, in some extent, contributed to the compatibility between phases—as shown by the shifting of the T_g of the parent polymers. We can deduce that at least two phases coexist (RFA-rich phase and rPET-rich phase), leading us to deduce that the blends formed a system with partial miscibility. Based on the T_g values and blend composition, we estimated the effectiveness degree (e_d) (Table 2). The calculation of this parameter involves the T_g value and the weight of each component in the blend. This allows us to infer the degree of interaction of the blend components [13, 15]. Both polymers showed that the degree of effectiveness increased as their contents decreased in blend. The highest values of e_d for rPET (18.44) and for RFA (13.73) were found for the blends RFA/rPET (80/20) and RFA/rPET (20/80), respectively. Considering that the variation of the T_g value was higher in these two blends, we may deduce that the interchange reactions occurred more significantly in these two blends.

TG/DTG

As shown before, blends of polycondensation polymers have been studied due to their academic and technological significance. There is relevance in understanding of the mutual influence of each polymer on thermal stability of polymer blends. Mendes and da Costa Pereira [37]

Table 1 T_g of RFA/rPET materials

Blends	T_g RFA phase/rPET phase/°C
100/0	16/–
80/20	18/56
50/50	18/62
20/80	22/64
0/100	–/66

Table 2 Effectiveness degree (e_d) of RFA/rPET materials

Blends RFA/rPET	e_d RFA	e_d rPET
100/0	–	–
80/20	4.40	18.44
50/50	6.75	4.77
20/80	13.73	3.45
0/100	–	–

published data on thermogravimetry of PET/PC blends. This blend showed at least two phases—one rich in PET and another rich in PC—that were detected, among other evidences, by the presence of two T_{max}. There was also a certain degree of compatibility, as a result of the acidolysis, alcoholysis and transesterification reactions occurred during the molten processing. In a recent article, Pires et al. [46] published data on the weathering of PET/PC (80/20 mass/mass%) melt extruded blend. For any exposure time, this blend showed two T_{max}, ascribed to the occurrence of two rich phases, PET and PC, respectively.

Figures 3 and 4 show the TG and DTG curves of the materials. Table 3 shows the data of thermal degradation temperatures—T_{20}, T_{max} and T_{final}. The degradation occurred at one step for neat materials, and two steps for the blends. Zo et al. [42] studied blends of polyamide-6 and thermoplastic polyurethane (PA-6/TPU, 90/10 and 80/20). The results on degradation temperatures revealed that TPU degraded at 300–400 °C and has lower thermal stability than PA-6. Herein, the T_{20} temperature represents the temperature in which all Spandex^{TM} was degraded. For the blends, the T_{max} was located between rPET and RFA, showing two values of temperature. The lowest temperature was ascribed to the rPET-rich phase, while the highest one was related to the RFA-rich phase. The reduction of T_{max} was assigned to the interchange reactions between RFA and rPET during the molten processing. As shown in Reactions Schemes 1–4 the reaction between internal RFA amide groups and rPET ester groups could be more likely to occur, but acidolysis, alcoholysis and/or aminolysis reactions between end groups and internal groups of RFA and rPET also contributed for the decay in the thermal stability of the blends.

^{1}H LFNMR

Figure 5 shows the ^{1}H LFNMR domain curves of the materials. For all samples, the relaxation times were in the range of 1–1000 ms. The RFA showed two domains: one with high mobility (1 ms) and another with low mobility (300–700 ms). The first domain was related to the absorbed water (hydrogen bond between water molecules and RFA carbonyl groups), because even when solidified from the melt, the presence of amide group in RFA allows the absorption of water [47–49]. The second one was ascribed to the mobility of the crystalline structure. The rPET showed three domains. One with high mobility (1–12 ms) was ascribed to the absorbed water (hydrogen bond between water molecules with rPET carbonyl groups). There was an intermediate domain (15–100 ms) showing high intensity and low mobility. The last domain (100–400 ms) was related to highly crystalline structure of the rPET. The blends behaved according to the weight of the components. The RAF/rPET (80/20 mass/mass%) blend showed three domains. The domains at (1–12 ms) and at (15–70 ms) were related to the rPET phase. It is interesting to mention that the molecular mobility of the second domain was reduced. This has happened probably due to the interchange reactions between RFA and rPET during the melt processing. The last domain occurred at (200–900 ms). It was broadened when compared to the RFA domain. This profile reinforces in some extent the existence of interchange reactions. Similar behaviour was observed in the RAF/rPET (50/50 mass/mass%) blend. The RAF/rPET (20/80) blend also showed three domains. The domains at (1–12 ms) and (15–70 ms) were considered as the contribution of the rPET phase. The third domain was

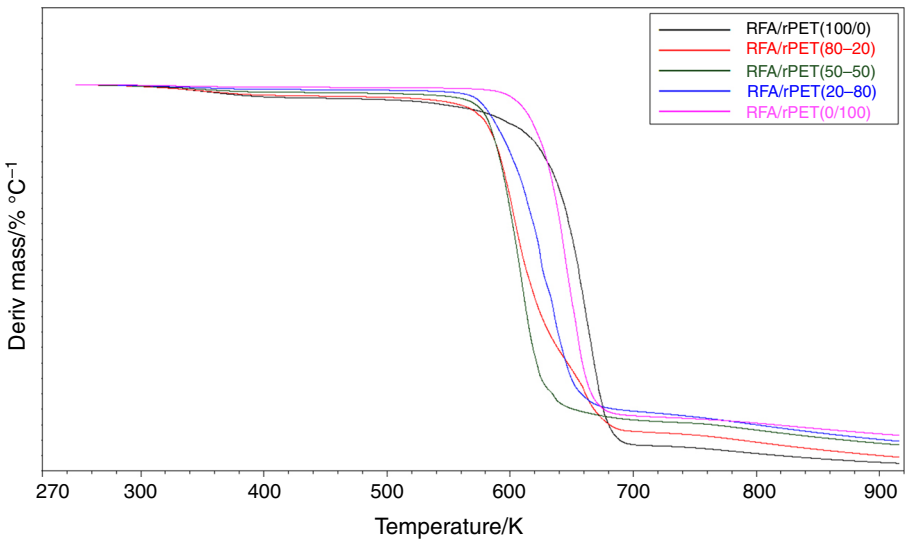

Fig. 3 TG curves of the blends RFA/rPET

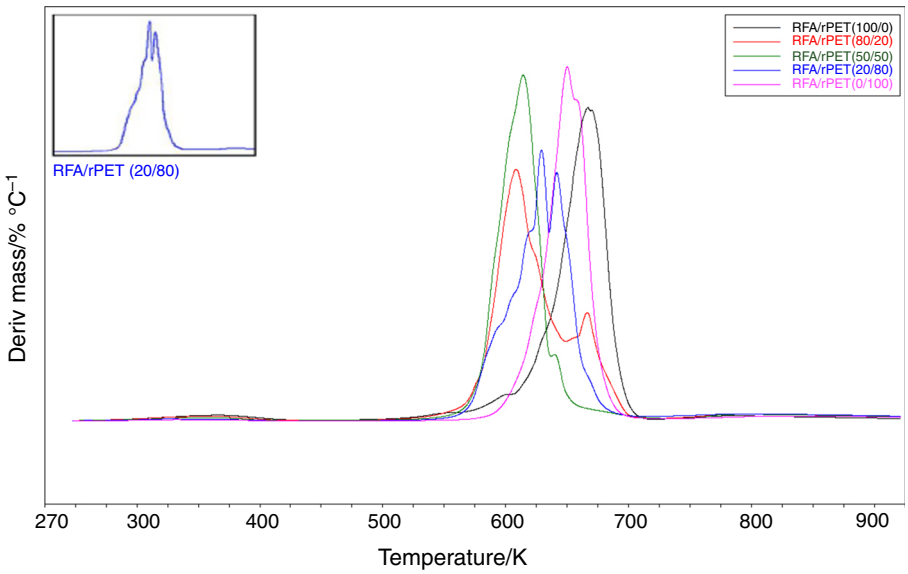

Fig. 4 DTG curves of the blends RFA/rPET

Table 3 TG/DTG properties of RFA/rPET materials

RFA/rPET	T_{20}/°C	T_{max}/°C rPET phase/RFA phase	Residue/%
100/0	410	–/444	9
80/20	373	383/441	8
50/50	372	389/415	7
20/80	384	404/416	4
0/100	411	435/–	2

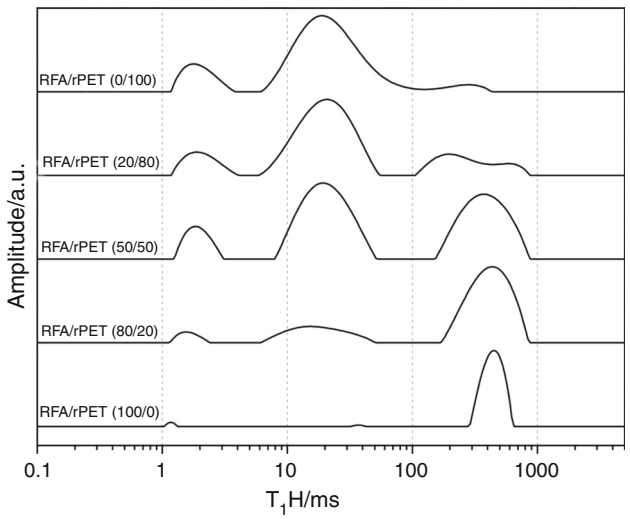

Fig. 5 ^{1}H LFNMR curves of RFA/rPET materials

split into two parts. The first one ranged (100–400 ms), and the second one was between (400–900 ms). Through this outline, we could deduce that there was some interaction between the RFA and rPET phases. The results reinforce even more the occurrence of interchange reactions and are in agreement with DMA and TG/DTG measurements.

DSC

The calorimetric curves of the second cycle of cooling and third cycle of heating are shown in Figs. 6 and 7. Table 4 shows the calorimetric data of these two cycles. Considering the blends, the RFA phase cooling crystallization temperature (T_{cc}) showed a slight decreasing tendency. There was no detectable trend in the variation of the rPET phase T_{cc} values. Concerning the melting temperature (T_m), the RFA phase showed two melting peaks ascribed to different crystal sizes. In the blends, the T_m of the RFA phase decreased, indicating the formation of less perfect crystals. For the rPET phase, some blends showed two melting peaks, belonging to crystals with different dimensions. Evstatiev et al. [17] reported the influence of exchange reactions in the calorimetric properties of melt processing PET-PA-6 blends. The authors pointed out that some cooperative crystallization process was induced by some block copolymer generated in situ. In this work, the X_c varied according to the weight of the components in the blend. There was a mutual influence on the crystallization rate of each polymer, affecting the kinetics and diffusion during the crystallization process. As seen in the ^{1}H LFNMR section, the RAF/rPET (20/80 mass/mass%) blend revealed greater variation in the molecular mobility. Herein, this blend showed a sharper change in the X_c. We can assume that the occurrence of interchange reactions between RFA and rPET was highlighted in this blend composition, during the molten state.

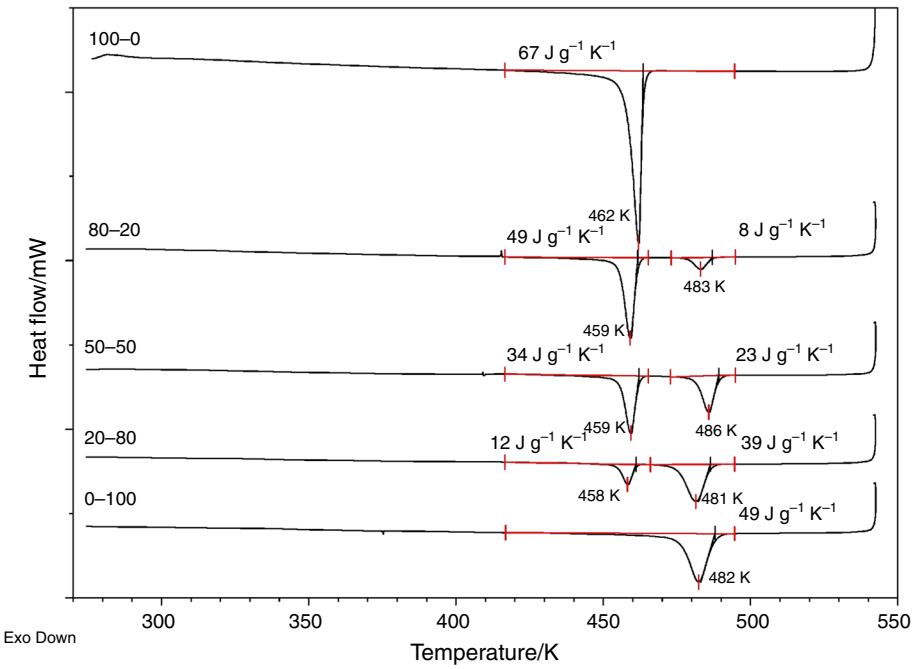

Fig. 6 Calorimetric curves of the samples (second cooling)

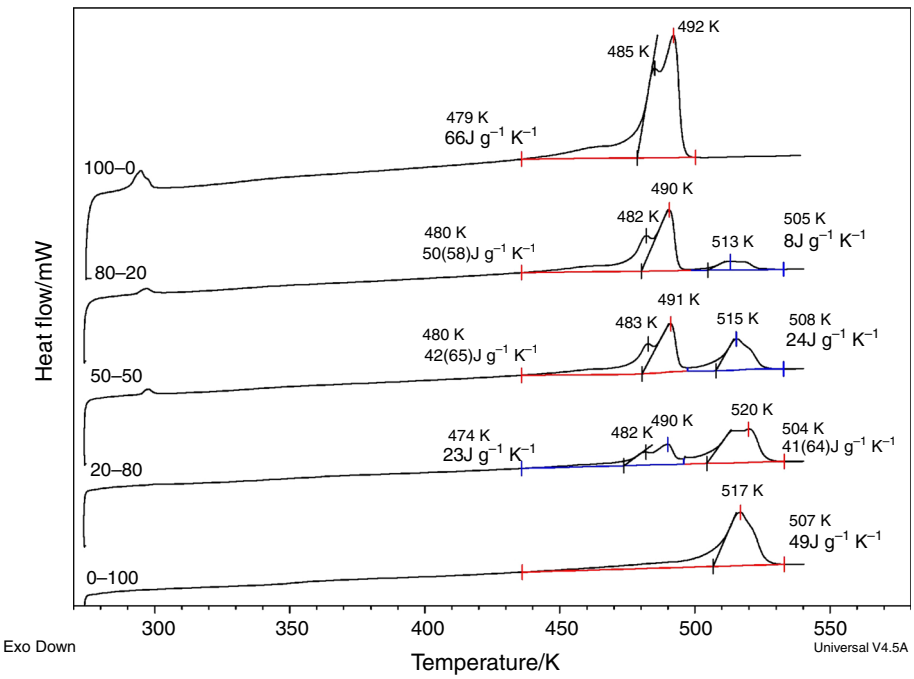

Fig. 7 Calorimetric curves of the samples (third heating)

Scanning electron of microscopy (SEM)

The choice for acetic acid as etching liquid was due to its action as solvent over the caprolactam monomer and PA-6 oligomers [27, 28]. The SEM micrographs of the RFA/rPET blends after etching are shown in Fig. 8. The cryogenic fracture of the precursor polymers did not show any plastic deformation, although the surfaces are related to ductile material. The blends micrographs revealed high cohesion between RFA and rPET phases. A high compatibilization degree was achieved. After etching, we observed voids of different sizes and amounts along the surfaces. This was possibly due to the removal of copolymeric structures arisen from the interchange reactions

Table 4 Calorimetric properties of RFA/rPET materials

RFA/rPET Blend	T_{cc} RFA phase/°C	T_{cc} rPET phase/°C	T_m RFA phase/°C	T_m rPET phase/°C	X_c RFA phase/%	X_c rPET phase/%
100/0	189	–	212/219	–	38.6	–
80/20	186	210	209/217	240	36.6	29.4
50/50	186	213	210/218	242	49.1	35.3
20/80	185	208	209/217	247	67.2	37.7
0/100	–	209	–	244	–	36.0

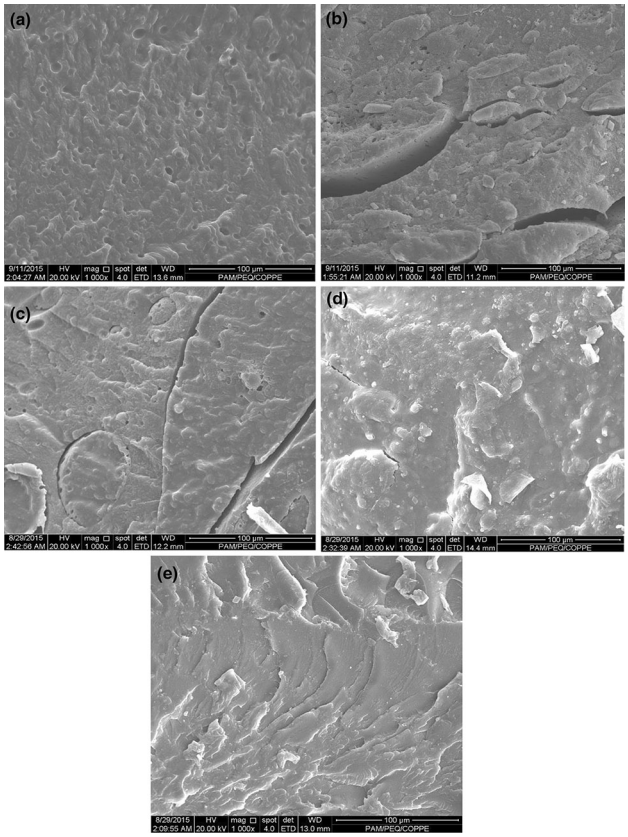

Fig. 8 SEM micrographs of RFA/rPET blends, after acid etching: **a** 100/0, **b** 80/20, **c** 50/50, **d** 20/80, **e** 0/100

between RFA and rPET, which acted as compatibilizing agent. The interfacial region of the blend RAF/rPET (20/80 mass/mass%) was less attacked, suggesting that the copolymeric structure formed during the molten processing is rich in rPET. The observed morphology reinforces the results of other analysis.

Mechanical analysis (stress–strain)

In Table 5 are listed the mechanical properties of the materials. The elastic modulus increased as function of rPET content, as reported by Ferreira et al. [50]. A synergistic effect was found for the RFA/rPET (20/80 mass/mass%) blend—the elastic modulus was higher than those of the precursor polymers. The stress at break showed decrease with the increase in rPET content. The values are lesser than half of neat RFA and rPET. The extremely low elongation of rPET implied in damage of the blend elongation. In fact, the elongation at break decreased drastically with the increase in the amount of rPET. Although the assumption of the occurrence of interchange reactions has been considered, their extent was not enough to improve some mechanical properties. Also, it is worth mentioning that alcoholysis, acidolysis and aminolysis reactions could be understood as degradative reaction. When interchange reactions succeed, a block copolymer chain is created and an oligomer chain of RFA or rPET is produced (see Reaction Schemes 1, 2, 3, 4). Their extent during the melt processing could have influenced the blend compatibility and properties.

Table 5 Mechanical properties of RFA/rPET materials

RFA/rPET Blend	Elastic modulus/MPa	Stress at break/MPa	Elongation at break/%
100/0	6.01	54.56	192.83
80/20	8.87	29.83	20.70
50/50	12.48	28.28	2.87
20/80	18.39	12.86	0.17
0/100	16.14	81.85	5.94

The results are concerned to the existence of interchange reactions. As shown in Reaction Schemes 1, 2, 3, and 4, the ester–amide reaction is a constructive reaction—two different copolymers are formed. With respect to the alcoholysis, acidolysis and aminolysis reactions, all of them can be considered degradative. One chain of copolymer and one oligomer are produced. The extent among them has influence on blend compatibility and properties.

Conclusions

In general, the thermal, molecular mobility, morphology and mechanical assessments were dependent on the weight fraction of each component in the blends. The variations on T_g, T_m, X_c and relaxation time strongly evidence the interchange reactions that has happened in the molten state. The extent of each reaction depended on the processing parameters. The reactive compatibilization performed during the blend preparation led to the achievement of a partially miscible blend.

Acknowledgements The authors strongly thank to Conselho Nacional de Desenvolvimento Científico e Tecnológico (CNPq), Coordenação do Aperfeiçoamento de Pessoal de Nível Superior (CAPES) and the Universidade Federal do Rio de Janeiro, for supporting this research.

References

1. Hu B, Serranti S, Fraunholcz N, Di Maio F, Bonifazi G. Recycling-oriented characterization of polyolefin packaging waste. Waste Manag. 2013;33(3):574–84.
2. Serranti S, Gargiulo A, Bonifazi G. Characterization of post-consumer polyolefin wastes by hyperspectral imaging for quality control in recycling processes. Waste Manag. 2011;31(11):2217–27.
3. Chaukura N, Gwenzi W, Bunhu T, Ruziwa DT, Pumure I. Potential uses and value-added products derived from waste polystyrene in developing countries: a review. Resour Conserv Recycl. 2016;107:157–65.
4. Urreaga JM, González-Sánchez C, Martínez-Aguirre A, Fonseca-Valero C, Acosta J, De la Orden M. Sustainable eco-composites obtained from agricultural and urban waste plastic blends and residual cellulose fibers. J Clean Prod. 2015;108:377–84.
5. Abit ABdITedC. Agenda de Prioridades Têxtil e Confecção – 2015/2018. São Paulo—Brazil. 2013. http://www.abit.org.br/conteudo/links/publicacoes/agenda_site.pdf. Accessed 16 Nov 2016.
6. Wang Y. Fiber and textile waste utilization. Waste Biomass Valoriz. 2010;1(1):135–43.
7. Mishra R, Behera B, Militky J. Recycling of textile waste into green composites: performance characterization. Polym Compos. 2014;35(10):1960–7.
8. Farrugia KJ, Bandey H, Dawson L, Daéid NN. Chemical enhancement of soil based footwear impressions on fabric. Forensic Sci Int. 2012;219(1):12–28.
9. Segatelli MG, Yoshida IVP, do Carmo Gonçalves M. Natural silica fiber as reinforcing filler of nylon 6. Compos B Eng. 2010;41(1):98–105.
10. Singha K. Analysis of spandex/cotton elastomeric properties: spinning and applications. Analysis. 2012;2(2):11–6.
11. Hamad K, Kaseem M, Deri F. Recycling of waste from polymer materials: an overview of the recent works. Polym Degrad Stab. 2013;98(12):2801–12.
12. Mendes LC, Pereira PSdC, Mallet IA, Cestari SP, Dias FGdA. Solid state polymerization of PET/PC extruded blend: effect of reaction temperature on thermal, morphological and viscosity properties. Polímeros. 2014.
13. Al-Jabareen A, Illescas S, Maspoch ML, Santana O. Effects of composition and transesterification catalysts on the physicochemical and dynamic properties of PC/PET blends rich in PC. J Mater Sci. 2010;45(24):6623–33.
14. Pereira PS, Mendes LC, Ramos VD, editors. Rheological study bringing new insights into PET/PC reactive blends. Macromolecular Symposia. Wiley Online Library; 2010.
15. Mendes LC, Pereira PS. Solid state polymerization: its action on thermal and rheological properties of PET/PC reactive blends. Polímeros. 2013;23(3):298–304.
16. Retolaza A, Eguiazabal J, Nazabal J. Structure and mechanical properties of polyamide-6,6/poly (ethylene terephthalate) blends. Polym Eng Sci. 2004;44(8):1405–13.
17. Evstatiev M, Petrovich S, Krasteva B. Calorimetric studies on PET/PA6 and PA66/PA6 drawn blends with various thermal histories. Bulg J Phys. 2003;30:70–9.
18. Denchev ZZ. In-situ composite materials based on oriented polymer blends: preparation, structure and properties. Devel Appl Pol Sci. 2006;3:119–41.
19. D3418 A. standard test method for transition temperatures and enthalpies of fusion and crystallization of polymers by differential scanning calorimetry. ASTM International; 2015.
20. Freitas DFS, Mendes LC, Lino AS. Polyamide-6/organointercalated lamellar zirconium phosphate nanocomposites: molecular mobility, crystallography and thermo-mechanical evaluation. J Nanosci Nanotechnol. 2016;17(5):3042–50.
21. Zuo J, Li S, Bouzidi L, Narine SS. Thermoplastic polyester amides derived from oleic acid. Polymer. 2011;52(20):4503–16.
22. Lips P, Broos R, Van Heeringen M, Dijkstra P, Feijen J. Synthesis and characterization of poly (ester amide) s containing crystallizable amide segments. Polymer. 2005;46(19):7823–33.
23. Son BT, Trung NN, Lim D-G, Shin S, Bae J-Y. Improvements in thermal, mechanical, and dielectric properties of epoxy resin by chemical modification with a novel amino-terminated liquid-crystalline copoly (ester amide). React Funct Polym. 2012;72(8):542–8.
24. Utracki L, Favis B. Polymer alloys and blends. New York: Marcel Dekker; 1989.
25. Fox TG. Influence of diluent and of copolymer composition on the glass temperature of a polymer system. Bull Am Phys Soc. 1956;1(2):123–35.
26. Santana O, Maspoch ML, Martinez A. Polycarbonate/acrylonitrile–butadiene–styrene blends: miscibility and interfacial adhesion. Polym Bull. 1998;41(6):721–8.
27. Pogorzelska Z, Mielniczuk Z. Determination of ε-caprolactam migration from polyamide plastics: a new approach. Pack Technol Sci. 2001;14(1):31–5.
28. Jiang L, Kong W, Wu B, Fu X, Xiao Y, Zhou C. Reactive processing of thermoplastic elastomers based on polyamide-6: preparation and characterization. Iran Polym J. 2016;25(9):765–73.
29. ASTM-D882. Standard test method for tensile properties of thin plastic sheeting. ASTM International; 2012.
30. Scheirs J. Compositional and failure analysis of polymers: a practical approach. Chichester: Wiley; 2000. p. 196.
31. Liu N, Huang H. 2 Types of reactive polymers used in blending. 2001.
32. Pircheraghi G, Nazockdast H, Salehi M. Effect of nanoclay surface modifier chemical reactivity on morphology and rheological properties of PP/PA6 Blend nanocomposite. Int Polym Proc. 2013;28(4):354–60.
33. Litmanovich AD, Platé NA, Kudryavtsev YV. Reactions in polymer blends: interchain effects and theoretical problems. Prog Polym Sci. 2002;27(5):915–70.
34. Samperi F, Montaudo M, Puglisi C, Alicata R, Montaudo G. Essential role of chain ends in the Ny6/PBT exchange. A combined NMR and MALDI approach. Macromolecules. 2003;36(19):7143–54.

35. Puglisi C, Samperi F, Di Giorgi S, Montaudo G. Exchange reactions occurring through active chain ends. MALDI-TOF characterization of copolymers from nylon 6, 6 and nylon 6, 10. Macromolecules. 2003;36(4):1098–107.
36. Samperi F, Puglisi C, Alicata R, Montando G. Essential role of chain ends in the nylon-6/poly (ethylene terephthalate) exchange. J Polym Sci A Polym Chem. 2003;41(18):2778–93.
37. Mendes LC, da Costa Pereira PS. Optical microscopy as a tool to correlate morphology and thermal properties of extruded PET/PC reactive blends. Mater Sci Appl. 2011;2(08):1033.
38. Lee MS, Ha MG, Choi CN, Yang KS, Kim JB, Kim TH, et al. Encapsulation in poly (ethylene terephthalate)/polyamide-6/phenoxy ternary blends. Polym J. 2002;34(7):510–4.
39. Mendes L, Dias M, Rodrigues T. Chemical recycling of PET waste with multifunctional pentaerythrytol in the melt state. J Polym Environ. 2011;19(1):254–62.
40. Lv F, Yao D, Wang Y, Wang C, Zhu P, Hong Y. Recycling of waste nylon 6/spandex blended fabrics by melt processing. Compos B Eng. 2015;77:232–7.
41. Chiu HT, Chuang CY. The mechanical and rheological behavior of the PA/TPU blend with POE-g-MA modifier. J Appl Polym Sci. 2010;115(3):1278–82.
42. Zo HJ, Joo SH, Kim T, Seo PS, Kim JH, Park JS. Enhanced mechanical and thermal properties of carbon fiber composites with polyamide and thermoplastic polyurethane blends. Fibers Polym. 2014;15(5):1071–7.
43. Zhou S, Huang J, Zhang Q. Mechanical and tribological properties of polyamide-based composites modified by thermoplastic polyurethane. J Thermoplast Compos Mater. 2012;27(1):18–34.
44. John B, Motokucho S, Kojio K, Furukawa M. Polyamide 6 fibers with superior mechanical properties: TPU coating techniques. Sen'i Gakkaishi. 2009;65(9):236–40.
45. Genovese A, Shanks R. Simulation of the specific interactions between polyamide-6 and a thermoplastic polyurethane. Comput Theor Polym Sci. 2001;11(1):57–62.
46. Pires HM, Mendes LC, Cestari SP, Pita VJRR. Effect of weathering and accelerated photoaging on PET/PC (80/20 wt/wt%) melt extruded blend. Mat Res. 2015;18(4):763–8.
47. Puffr R, Šebenda J, editors. On the structure and properties of polyamides. XXVII. The mechanism of water sorption in polyamides. J Polym Sci C Polym Symp; 1967. Wiley Online Library.
48. Choi YJ, Kim SH. Characterization of recycled polyethylene terephthalates and polyethylene terephthalate–nylon6 blend knitted fabrics. Text Res J. 2015;85(4):337–45.
49. Bouma K, De Wit G, Lohmeijer J, Gaymans R. Polyesteramides based on PET and nylon 2, T part 3. Properties. Polymer. 2000;41(11):3965–74.
50. Ferreira CT, Perez CA, Hirayama D, Saron C. Recycling of polyamide (PA) from scrap tires as composites and blends. J Environ Chem Eng. 2013;1(4):762–7.